Supplementary Information for

Melting of Charge Density Waves in Low Dimensions

Jeremy M. Shen[1], Alex Stangel[2], Suk Hyun Sung[3], Nishkarsh Agarwal[2], Ismail El Baggari[3], Kai Sun[4], and Robert Hovden[2,4,*]

[1]Department of Electrical and Computer Engineering, University of Michigan, Ann Arbor, MI. [2]Department of Materials Science and Engineering, University of Michigan, Ann Arbor, MI. [3]The Rowland Institute at Harvard, Cambridge, MA. [4]Department of Physics, University of Michigan, Ann Arbor, MI. [*]e-mail: hovden@umich.edu

1 Melting with Volume Reduction and Charge Relaxation

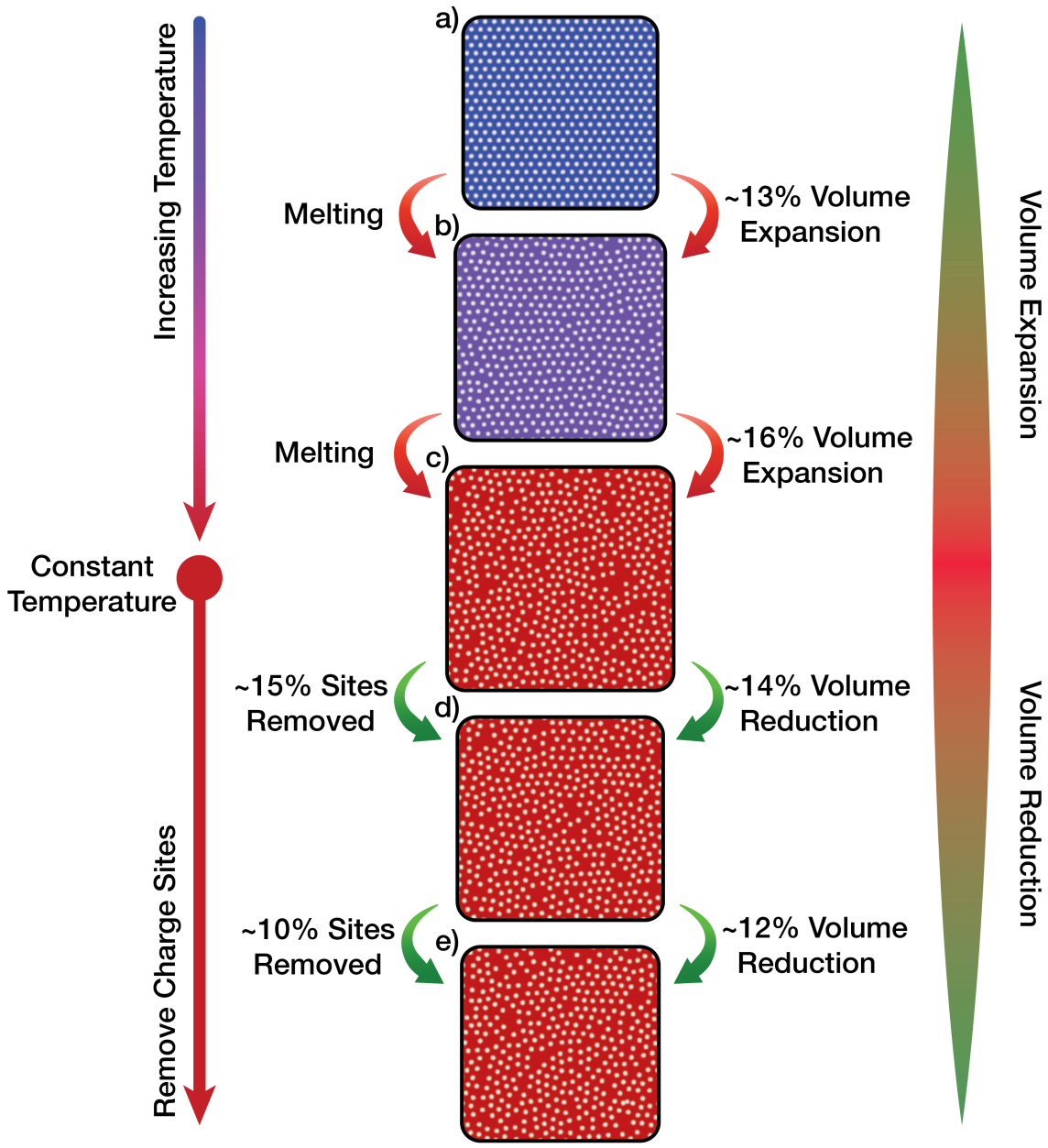

Supplementary Figure 1 | Melting of 2D Crystal with Volume Expansion and Charge Removal. a–c) Classical melting of 2D crystal with volume expansion. Topological defects occupy increased volume, driving an increased average lattice spacing. CDW amplitude collapses near topological sites. In the discrete charge crystal representation, amplitude collapse is modeled as the removal of charge centers. At constant temperature and pressure, reducing particle count accommodates a volume reduction **(c–e)**. The volume of melted state **(e)** is equal to that of the ordered state **(a)**, and there is a 23% site reduction. The reduction in particle count at a fixed volume increases the average lattice spacing.

2 Extended Meta-Analysis on CDW Melting

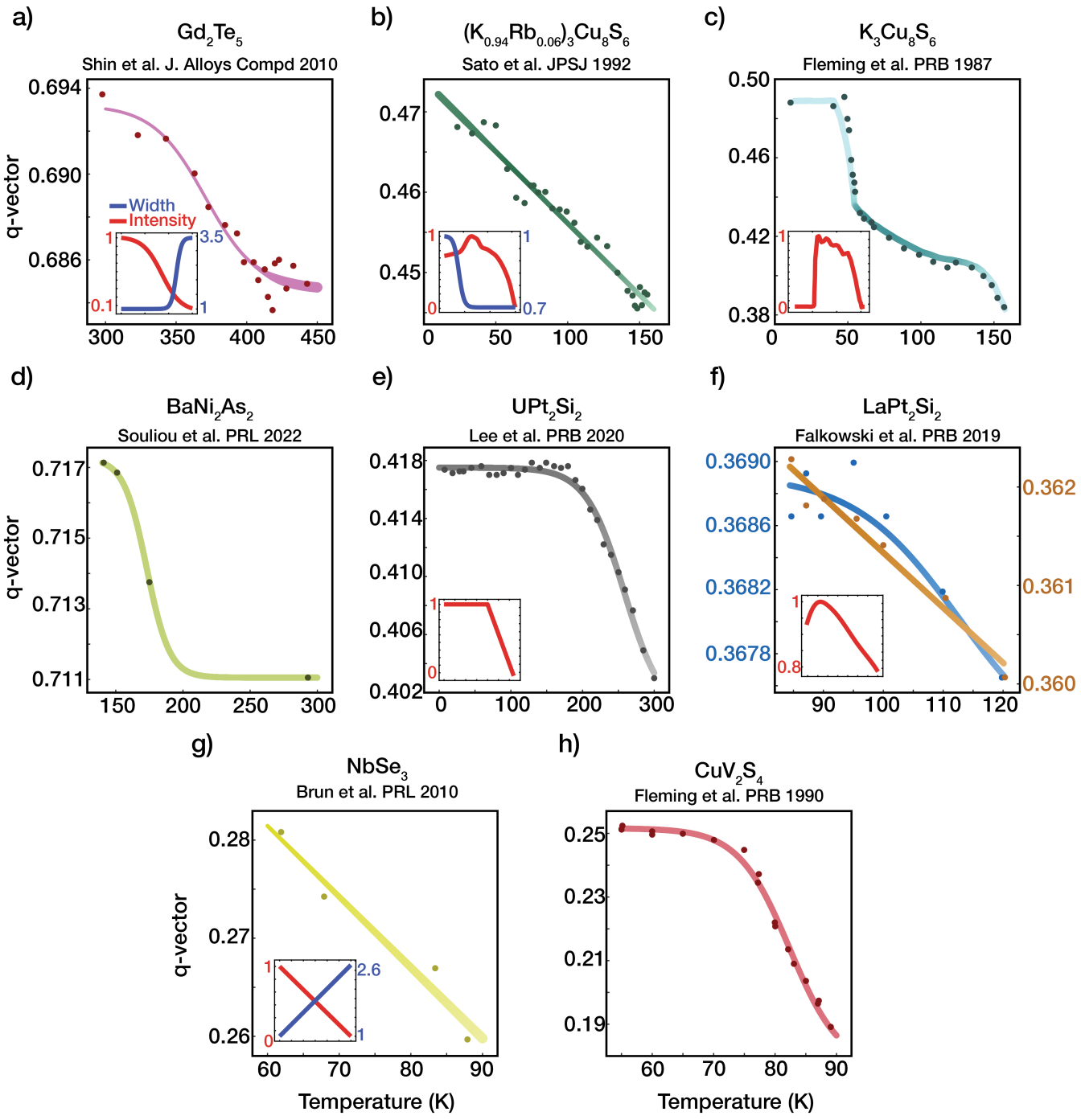

Supplementary Figure 2 | Melting of 2D CDWs. Wavevector contraction is present in layered tellurides[1] **a)**, 2D metals[2,3] **b,c)**, and other anisotropic, layered materials[4–6] **d–f)**. The 2D CDW in $NbSe_3$ and 3D (quasi-2D) CDW in CuV_2S_4 also report wavevector contraction[7,8]. Onset of the CDW is sometimes reported **(b, c)**, hence the initial increase in integrated intensity. **b)** Surprisingly, the width of the superlattice peak actually decreases. **f)** Falkowski et al. reports differences in measured wavevector for the positive +q (left, blue) and negative −q (right, gold). Fitted lines are guides to the eye, where line width and color intensity is proportional to CDW peak width and integrated intensity respectively (if reported).

3 Extended Meta-Analysis on CDW Melting in Manganites

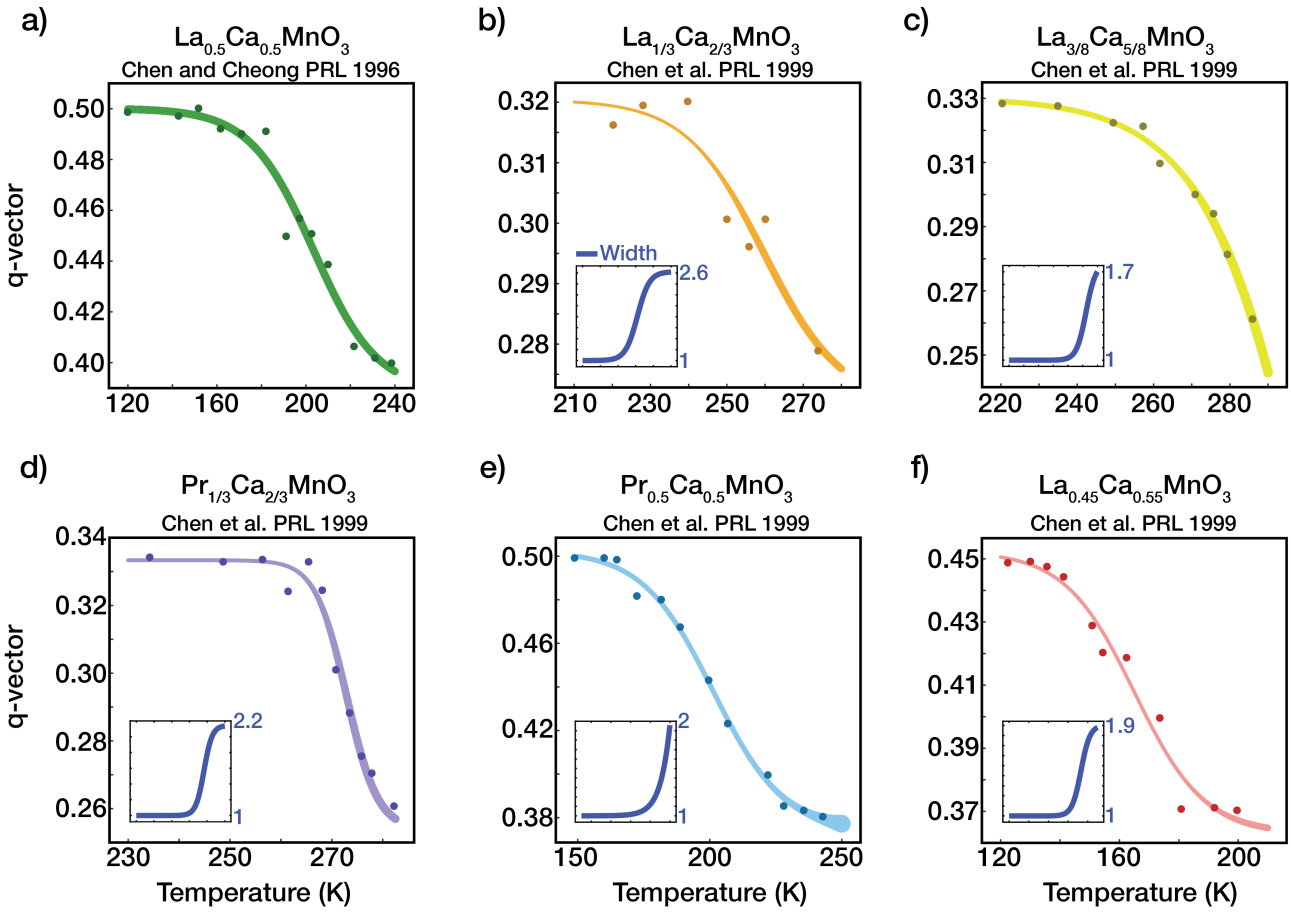

Supplementary Figure 3 | Melting of 2D CDWs in Manganites. a–f) CDW melting in manganites from[9–11]. All reported manganite systems melt with a wavevector contraction and, when provided, azimuthal blurring of the peaks. Fitted lines are guides to the eye, where line width and color intensity is proportional to CDW peak width and integrated intensity respectively (if reported).

4 Extended Meta-Analysis on 1D CDW Melting

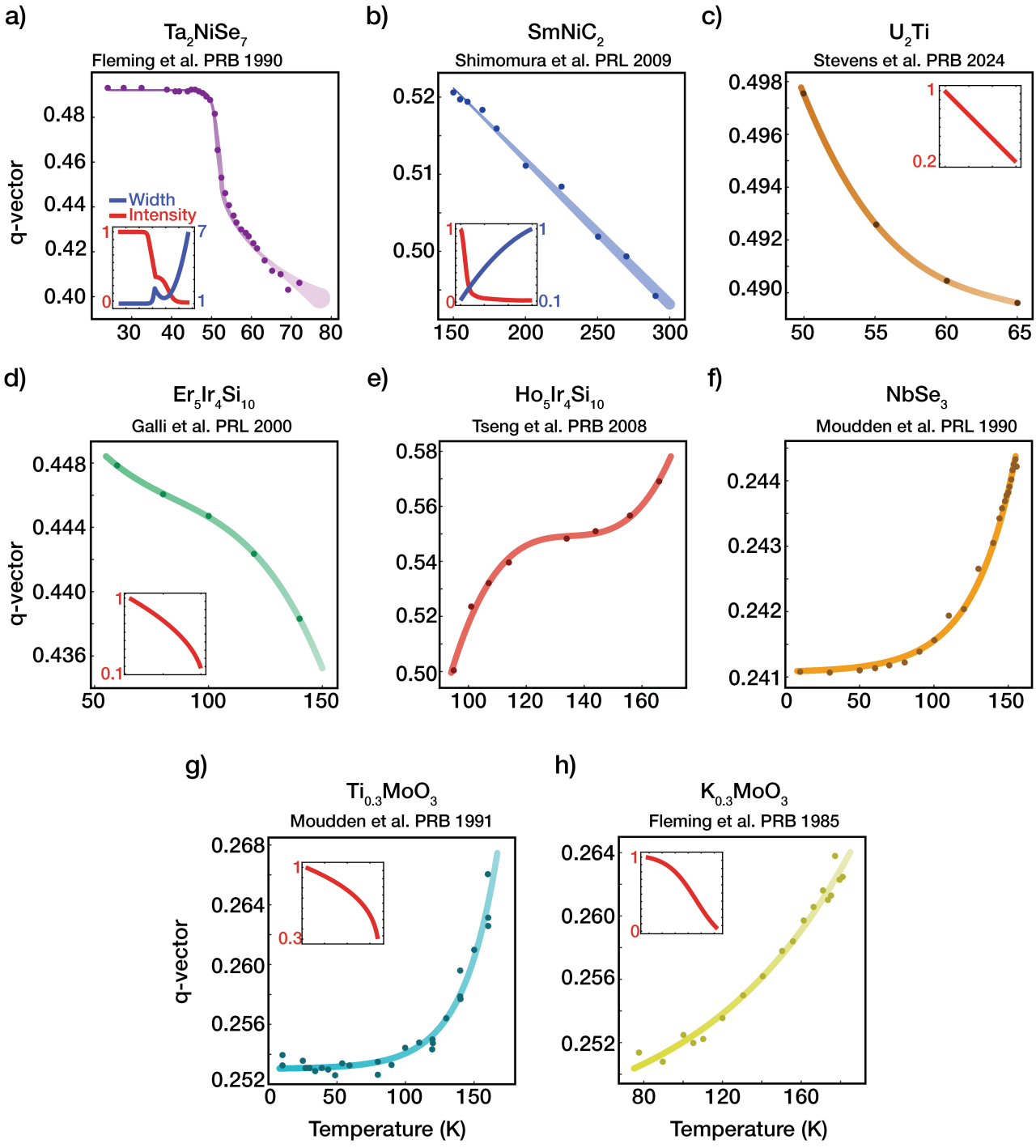

Supplementary Figure 4 | Melting of 1D CDWs. a–c) Wavevector contraction is oberved in 1D CDW systems Ta_2NiSe_7, $SmNiC_2$, and U_2Ti[12–14]. The 1D CDW wavevctor in ternary rare-earth metal silicides $R_5Ir_4Si_10$ contract with R=Er[15] **(d)** and expand with R=Ho[16] **(e)**. Wavevector expansion is reported in the 1D CDW in $NbSe_3$[17] **(f)** and blue bronzes[18,19] **g–h)**. Regardless of wavevector evolution direction, the peak width increases and the integrated intesnity decreases. Fitted lines are guides to the eye, where line width and color intensity is proportional to CDW peak width and integrated intensity respectively (if reported).

5 Wavevector Contraction in Reduced Directions

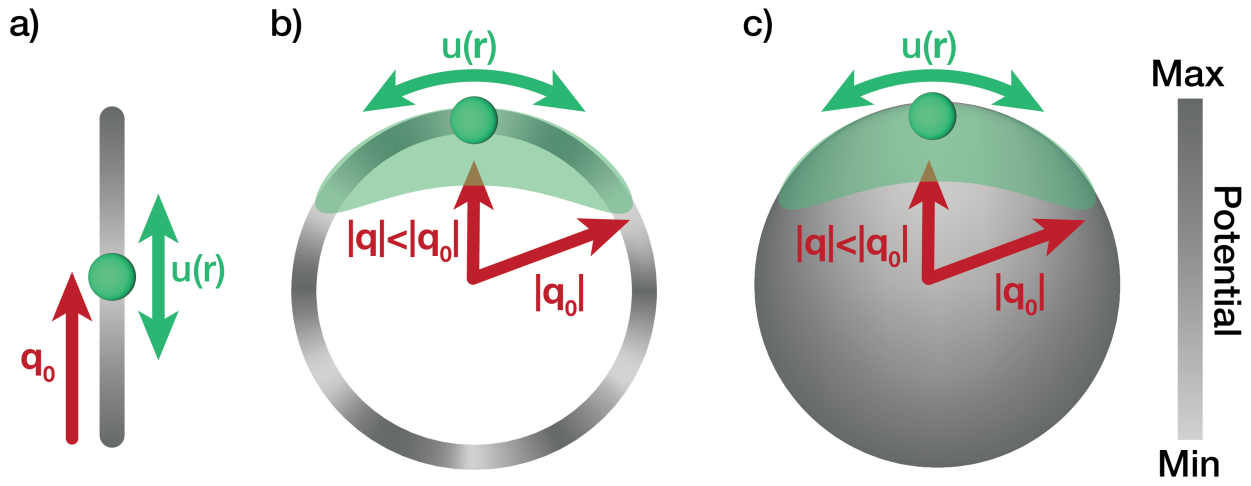

Supplementary Figure 5 | Fluctuation Effects on Wavevector in Reduced Dimensions. Reciprocal space potential landscape and wavevector behavior in **(a)** 1-, **(b)** 2-, and **(c)** 3- dimensions. The principal wavevector $\mathbf{q_0}$ sits at the minimum in the free energy. In 1D, fluctuations of the phase, $u(r)$, induce no preference for the evolution of the wavevector. Higher dimensionalities introduce convexity in the potential landscape. Fluctuations of the phase, $u(\mathbf{r})$ in 2D (3D) about the minimum create oscillations along a ring (sphere) of radius $\mathbf{q_0}$. Discrete rotational symmetry prevents $\mathbf{q}$ from rotating. Rather, the wavector smears azimuthally and contracts.

6 Liquid Crystal Melting and Continuous Rotational Symmetry

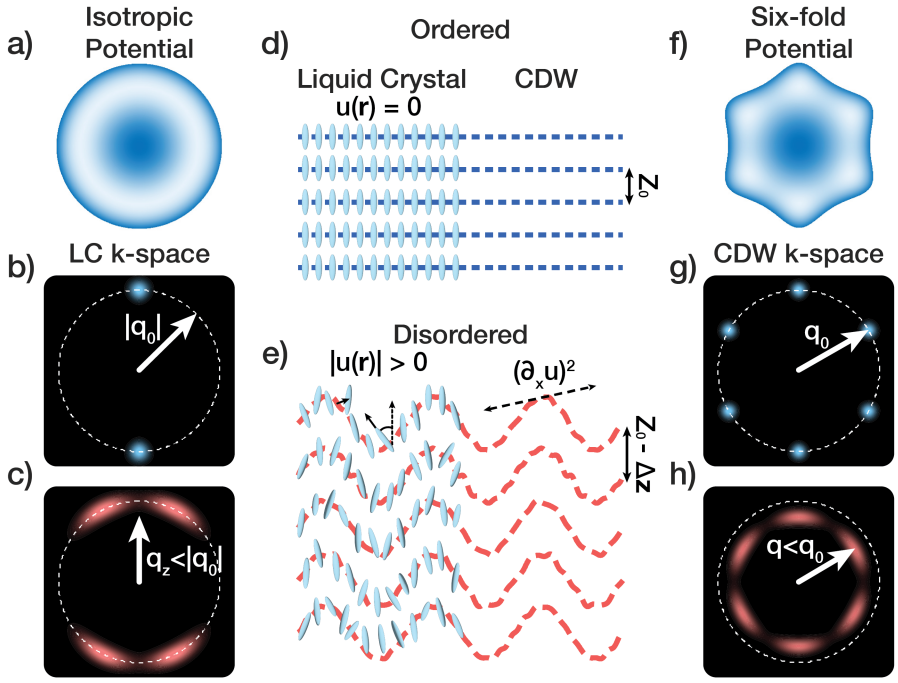

Supplementary Figure 6 | Melting of density wave in continuous and discrete rotational potentials. Potential landscape with continuous **(a)** and discrete **(f)** rotational symmetry. **d, e)** Melting of liquid crystals (left) and CDWs (right) couple disorder in wavefront to wavelength. Ordered **(b)** and disordered **(c)** liquid crystal in k-space. The liquid crystal is free to rotate along the energy minima, and the peak in k-space splits. **g, h)** There is a high energy cost for the CDW to rotate so the peak moves in and smears instead.

7 CDW Melting Observed in the Atomic Lattice

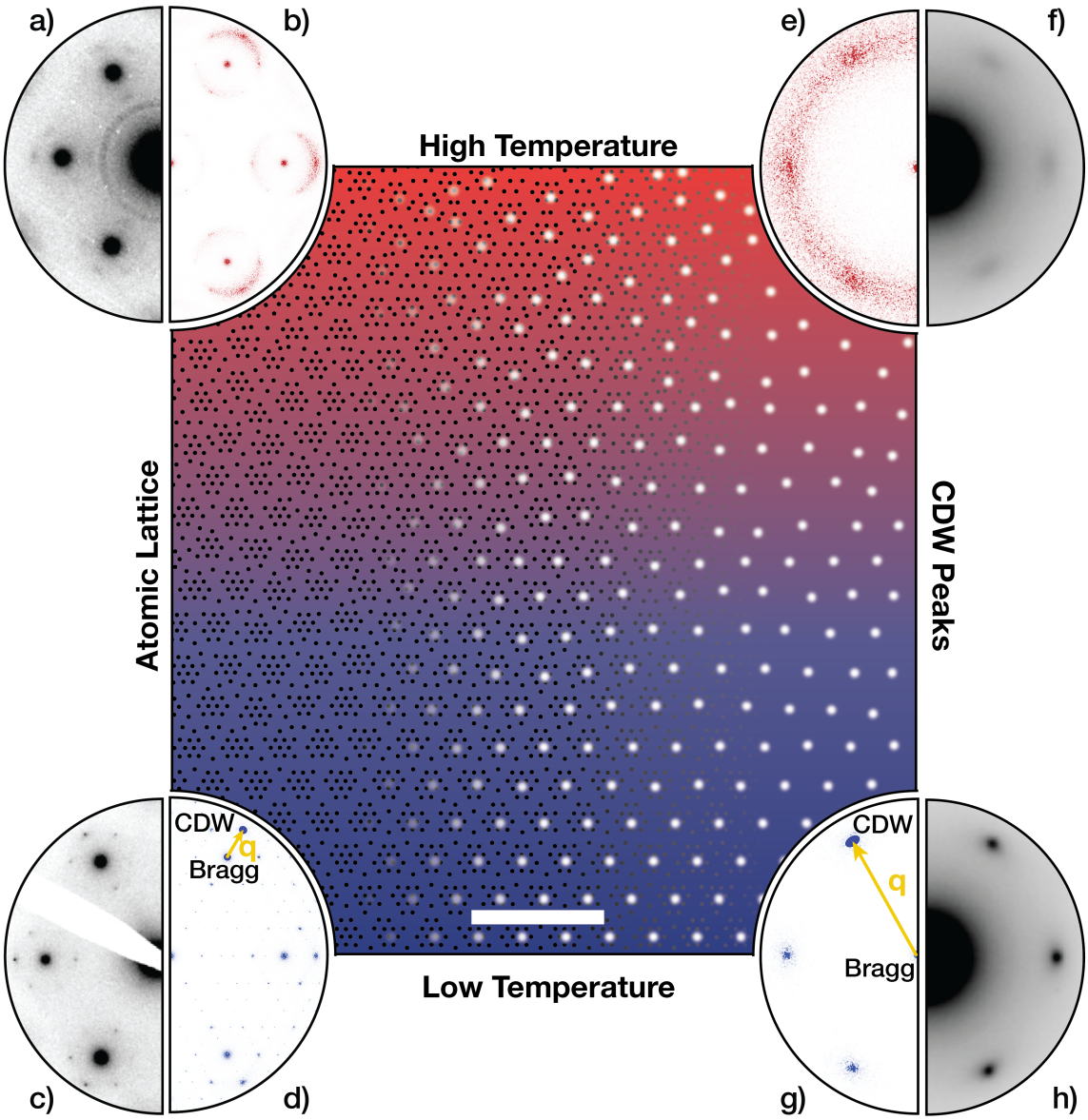

Supplementary Figure 7 | Melting of CDW in an Atomic Lattice. Tantalum nuclei (black spots, left) positions modulated by a progressively melted CDW (CDW peaks as white spots, right). Scale bar is 5nm. The charge lattice, too, becomes progressively disordered. The atomic lattice remains ordered but disorder manifests in the associated periodic lattice distortions. Here, the periodic lattice distortion effect is exaggerated for visual clarity. Comparison of 2D 1T-TaS_2 diffraction pattern **(a, c)** with simulated atomic lattice **(b, d)** at low and high temperatures. The **q**-vector points from the Bragg peak to the CDW superlattice peaks. The superlattice peaks are anisotropically distributed around each Bragg peak. Averaging the six first order Bragg peaks and surrounding superlattice peaks removes the anisotropy and serves as a direct probe of the CDW **(f, h)**. Simulated diffraction of the CDW peaks matches experimental CDW melting.

8 Free Energy of a Unidirectional CDW with 6-Fold Rotational Symmetry

For a two-dimensional system with discrete 6-fold rotational symmetry system which orders along one dimension at $|\mathbf{q}| = q_0$, the free energy can be given by[20]:

$$H = \frac{1}{2}K\int d^2r\left\{-2q_0^2\left[\nabla m(\mathbf{r})\right]^2 + \left[\nabla^2 m(\mathbf{r})\right]^2\right\} + W\int d^2r\left\{\left[\left(\partial_x^3 - 3\partial_x\partial_z^2\right)m(\mathbf{r})\right]^2\right\} \tag{1}$$

where $m(\mathbf{r}) = \mathrm{Re}\{\psi(\mathbf{r})\}$ is the real part of the system's order parameter $\psi(\mathbf{r}) = A(\mathbf{r})\exp[iq(z+u(\mathbf{r}))]$. $qu(\mathbf{r})$ are fluctuations of the phase. Fluctuations in the amplitude will be neglected ($A(\mathbf{r}) = A$) as we are focusing on fluctuating displacements of the wavefront ($u(\mathbf{r})$) which are prevalent in 2D CDW melting. Notably, we modify the free energy by including a sixth-order term in m:

$$\left(\partial_x^3 - 3\partial_x\partial_z^2\right)m(\mathbf{r}). \tag{2}$$

This term encodes the six-fold rotational symmetry of our system, creating an energy landscape in Fourier space as $q^6\cos(6\theta)$ (Fig. 4f).
Expanding the terms in the first integral individually we find that

$$-2q_0^2\left[\nabla m(\mathbf{r})\right]^2 = -A^2\left\{\underline{q_0^2q^2\left[(\partial_x u)^2 + (\partial_z u)^2\right]} + \underline{q_0^2q^2} + \underline{2q_0^2q^2\partial_z u}\right\}, \tag{3}$$

and

$$\begin{aligned}\left[\nabla^2 m(\mathbf{r})\right]^2 = A^2\Big\{&\underline{\frac{1}{2}q^4} + \underline{\frac{1}{2}q^4\left(\partial_x u\right)^4} + \underline{q^4\left(\partial_z u\right)^2} + \underline{q^4\left(\partial_x u\right)^2} + \underline{2q^4\left(\partial_z u\right)} + \underline{2q^4\left(\partial_z u\right)^2} + \underline{2q^4\partial_z u\left(\partial_x u\right)^2}\\ &+ \underline{\frac{1}{2}q^2\left(\partial_x^2 u\right)^2} + \frac{1}{2}q^2\left(\partial_z^2 u\right)^2 + \frac{1}{2}q^4\left(\partial_z u\right)^4 + 2q^4\left(\partial_z u\right)^3 + q^4\left(\partial_x u\right)^2\left(\partial_z u\right)^2 + +q^2\left(\partial_x^2 u\right)\left(\partial_z^2 u\right)\Big\}.\end{aligned} \tag{4}$$

Note here that we have averaged over one period such that $\cos^2(qz + qu(\mathbf{r}))$ and $\sin^2(qz + qu(\mathbf{r}))$ average to $\frac{1}{2}$ and $\cos(qz + qu(\mathbf{r}))\sin(qz + qu(\mathbf{r}))$ average to zero. Further, all underlined terms are those which are kept in the expansion as we neglect higher-order terms such as $(\partial_z u)^4, (\partial_z u)^3, (\partial_z^2 u)^2$ and $(\partial_z u)^2(\partial_x u)^2$ since these do not affect the long-range behavior of our system[20,21]. Grouping these remaining terms together we have:

$$\begin{aligned}H = \frac{1}{2}KA^2\int d^2r\Big\{&q^4\left[\frac{1}{2} - \frac{q_0^2}{q^2}\right] + 2q^4\left[(\partial_z u) - q^{-2}q_0^2\left(\partial_z u\right)\right] + q^4\left[(\partial_x u)^2 + (\partial_z u)^2 - q^{-2}q_0^2\left((\partial_x u)^2 + (\partial_z u)^2\right)\right]\\ &+ \frac{q^2}{2}\left[\left(\partial_x^2 u\right)^2\right] + 2q^4\left[\left(\partial_z u\right)^2\right] + 2q^4\left[\partial_z u\left(\partial_x u\right)^2\right] + \frac{q^4}{2}\left[\left(\partial_x u\right)^4\right]\Big\}.\end{aligned} \tag{5}$$

Assuming the wavevector q will shift negligibly, we can set $q = q_0$:

$$H = \frac{1}{2}KA^2q_0^4\int d^2r\left\{C_0\left(\partial_x u\right)^2 + \frac{1}{2q_0^2}\left(\partial_x^2 u\right)^2 + 2\left(\partial_z u\right)^2 + 2\partial_z u\left(\partial_x u\right)^2 + \frac{1}{2}\left(\partial_x u\right)^4\right\}. \tag{6}$$

Note we have dropped the constant term $-\frac{1}{2}q_0^4$ in H since it does not affect any conclusions on the behavior of our system. We will now determine the factor C_0. To start, we expand $\left(\partial_x^3 - 3\partial_x\partial_z^2\right)m(\mathbf{r})$, neglecting any terms of order $O(u^3)$ and higher. This leaves us with

$$\begin{aligned}\left(\partial_x^3 - 3\partial_x\partial_z^2\right)m(\mathbf{r}) = A^2\big\{&18q_0^4(\partial_x\partial_z u)^2 + \underline{\frac{9}{2}q_0^6(\partial_x u)^2} + \frac{1}{2}q_0^2(\partial_x^3 u)^2 + \frac{9}{2}q_0^2(\partial_x\partial_z^2 u)^2 - 9q_0^4(\partial_x u)(\partial_x\partial_z^2 u)\\ &+ 3q_0^4(\partial_x u)(\partial_x^3 u) - 3(\partial_x\partial_z^2 u)(\partial_x^3 u)\big\} + O(u^3).\end{aligned} \tag{7}$$

Further, we will only keep the lowest order term, $(\partial_x u)^2$ (underlined), since this is the term of interest and all other terms are of higher order:

$$\left(\partial_x^3 - 3\partial_x\partial_z^2\right)m(\mathbf{r}) = A^2\frac{9}{2}q_0^6(\partial_x u)^2 + \text{higher order terms} \tag{8}$$

This term represents a correction to the $(\partial_x u)^2$ term induced by the six-fold symmetry of our system. With this correction we have for C_0:

$$C_0 = \frac{1}{q_0^2}\left(\frac{K}{2}q_0^2 - \frac{K}{2}q_0^2 + W\frac{9}{2}q_0^4\right) = W\frac{9}{2}q_0^2. \tag{9}$$

We note that, aside from $(\partial_z u)$, other coefficients of the terms in the expansion will also have similar corrections. We neglect these corrections as they do not cause the system's behavior to deviate from that of the system with continuous rotational symmetry. With these corrections we return to the final expression from the main text:

$$H = \frac{1}{2} K A^2 q_0^4 \int d^2 r \left\{ C_0 (\partial_x u)^2 + \frac{1}{2q_0^2} (\partial_x^2 u)^2 + 2(\partial_z u)^2 + 2\partial_z u (\partial_x u)^2 + \frac{1}{2}[(\partial_x u)^2]^2 + \text{higher order terms} \right\} \tag{10}$$

References

1. Shin, K. Y. *et al.* Observation of two separate charge density wave transitions in Gd_2Te_5 via transmission electron microscopy and high-resolution X-ray diffraction. *J. Alloys Compd.* **489,** 332–335 (2010).
2. Fleming, R. M., ter Haar, L. W. & DiSalvo, F. J. X-ray scattering study of charge-density waves in $K_3Cu_8S_6$. *Phys. Rev. B* **35,** 5388–5391 (1987).
3. Sato, H., Kojima, N. & Kagoshima, S. Structural Phase Transitions of the Quasi Two-Dimensional Metal $(K_{1-x}Rb_x)Cu_8S_6$: X-Ray Scattering Studies. *J. Phys. Soc. Japan* **62,** 2051–2061 (1993).
4. Souliou, S. M. *et al.* Soft-Phonon and Charge-Density-Wave Formation in Nematic $BaNi_2As_2$. *Phys. Rev. Lett.* **129,** 247602 (2022).
5. Lee, J. *et al.* Charge density wave with anomalous temperature dependence in UPt_2Si_2. *Phys. Rev. B* **102,** 041112 (2020).
6. Falkowski, M., Doležal, P., Andreev, A. V., Duverger-Nédellec, E. & Havela, L. Structural, thermodynamic, thermal, and electron transport properties of single-crystalline $LaPt_2Si_2$. *Phys. Rev. B* **100,** 064103 (2019).
7. Brun, C., Wang, Z.-Z., Monceau, P. & Brazovskii, S. Surface Charge Density Wave Phase Transition in $NbSe_3$. *Phys. Rev. Lett.* **104,** 256403 (2010).
8. Fleming, R. M., DiSalvo, F. J., Cava, R. J. & Waszczak, J. V. Observation of charge-density waves in the cubic spinel structure CuV_2S_4. *Phys. Rev. B* **24,** 2850–2853 (1981).
9. Chen, C. H. & Cheong, S.-W. Commensurate to Incommensurate Charge Ordering and Its Real-Space Images in $La_{0.5}Ca_{0.5}MnO_3$. *Phys. Rev. Lett.* **76,** 4042–4045 (1996).
10. Chen, C. H., Mori, S. & Cheong, S.-W. Anomalous Melting Transition of the Charge-Ordered State in Manganites. *Phys. Rev. Lett.* **83,** 4792–4795 (1999).
11. Milward, G. C., Calderón, M. J. & Littlewood, P. B. Electronically soft phases in manganites. *Nature* **433,** 607–610 (2005).
12. Fleming, R. M., Sunshine, S. A., Chen, C. H., Schneemeyer, L. F. & Waszczak, J. V. Defect-inhibited incommensurate distortion in Ta_2NiSe_7. *Phys. Rev. B* **42,** 4954–4959 (1990).
13. Shimomura, S. *et al.* Charge-Density-Wave Destruction and Ferromagnetic Order in $SmNiC_2$. *Phys. Rev. Lett.* **102,** 076404 (2009).
14. Stevens, C. R., Hermann, A., Huxley, A. & Wermeille, D. Incommensurate charge density wave order in U_2Ti. *Phys. Rev. B* **109,** 125116 (2024).
15. Galli, F. *et al.* Charge-Density-Wave Transitions in the Local-Moment Magnet $Er_5Ir_4Si_{10}$. *Phys. Rev. Lett.* **85,** 158–161 (2000).
16. Tseng, C. M., Chen, C. H. & Yang, H. D. Direct observation of charge-density waves in $Ho_5Ir_4Si_{10}$. *Phys. Rev. B* **77,** 155131 (2008).
17. Moudden, A. H., Axe, J. D., Monceau, P. & Levy, F. q_1 charge-density wave in $NbSe_3$. *Phys. Rev. Lett.* **65,** 223–226 (1990).
18. Moudden, A. H., Elmiger, M., Shapiro, S. M., Collins, B. T. & Greenblatt, M. Neutron-scattering investigation of the charge-density wave in $Tl_{0.3}$MoO3. *Phys. Rev. B* **44,** 3324–3327 (1991).
19. Fleming, R. M., Schneemeyer, L. F. & Moncton, D. E. Commensurate-incommensurate transition in the charge-density-wave state of $K_{0.30}MoO_3$. *Phys. Rev. B* **31,** 899–903 (1985).
20. Grinstein, G. & Pelcovits, R. A. Anharmonic Effects in Bulk Smectic Liquid Crystals and Other "One-Dimensional Solids". *Phys. Rev. Lett.* **47,** 856–859 (1981).
21. Grinstein, G. & Pelcovits, R. A. Nonlinear elastic theory of smectic liquid crystals. *Phys. Rev. A* **26,** 915–925 (1982).